

This paper was published in Applied Optics and is made available as an electronic reprint with the permission of OSA. The paper can be found at the following URL on the OSA website: <http://www.opticsinfobase.org/abstract.cfm?URI=ao-36-3-735>. Systematic or multiple reproduction or distribution to multiple locations via electronic or other means is prohibited and is subject to penalties under law.

# Infrared spectroscopy of tropospheric trace gases: combined analysis of horizontal and vertical column abundances

Ralf Sussmann and Klaus Schäfer

Vibration-rotation absorptions in high-resolution Fourier-transform infrared spectra from a 246-m horizontal path were used to derive local concentrations of trace gases at the Alpine observatory at the Zugspitze summit, Germany (2964 m above sea level). The analysis was performed by using the line-by-line nonlinear least-squares spectral fitting software, SFIT, based on the 1992 HITRAN line parameter compilation. (HITRAN is a high-resolution transmission molecular absorption database.) A comparison to *in situ* measurements shows an agreement of better than 4.3% for the species CO, CO<sub>2</sub>, and CH<sub>4</sub>. Using the same spectrometer and analysis software, we obtained the vertical column density of N<sub>2</sub>O together with an adjusted vertical volume mixing ratio distribution. This translates to a local N<sub>2</sub>O concentration at the altitude of Zugspitze that agrees with the horizontal path-derived value to within 1%. © 1997 Optical Society of America

*Key words:* Remote sensing, Fourier-transform infrared spectroscopy, open path, *in situ*, solar absorption, vertical profile.

## 1. Introduction

During the past decade the very-high-resolution Fourier-transform infrared (FTIR) spectrometry of atmospheric trace gases, with an instrumental linewidth well below the molecular (Doppler and pressure broadened) linewidth, has reached a high-quality level, both experimentally and theoretically. Solar absorption measurements for monitoring the trends of trace-gas vertical columns are being performed at various sites around the globe, e.g., at the Jungfraujoch Station (Switzerland),<sup>1</sup> at Kitt Peak (Arizona),<sup>2</sup> in Antarctica<sup>3,4</sup> and Arctica,<sup>5</sup> and at Lauder (New Zealand).<sup>6</sup> Most groups perform the concentration analysis of the spectra based on the Lambert-Beer law using the SFIT fitting algorithm developed by Rinsland at NASA Langley Research Center, Hampton, Virginia, during the early 1980's, which has been steadily updated.<sup>2</sup> (SFIT is line-by-line nonlinear least-squares spectral fitting software.) Newest developments are to retrieve the vertical distribution of trace gases from the shape

of atmospheric absorption lines, as already reported for the examples of carbon monoxide,<sup>7</sup> ozone,<sup>8</sup> and hydrogen fluoride and hydrogen chloride.<sup>9</sup> In order to get an unambiguous result, the need for accurate monitoring of the contribution of the actual instrumental line shape (ILS) is well recognized.<sup>10</sup> Experimental approaches to this problem are currently being discussed.<sup>11</sup>

During 1995 an environmental high-altitude observatory with a FTIR spectrometer was built at the summit of Zugspitze (47.4 °N, 11 °E, 2964 m above sea level). The goal of the measurement program started recently is to monitor both local concentrations and zenith columns of trace gases at a clean rural site that is essentially undisturbed by local contaminations. Our goal is to report on new experimental techniques, initial results, and validations of different experimental options. The structure of the paper is as follows. After a description of the new experimental features (Section 2), we present an analysis of the 246-m open-path spectra of the trace gases CO, CO<sub>2</sub>, and CH<sub>4</sub> (Subsections 3.A and 3.B). In Subsection 3.C we compare *in situ* measurements of these species performed regularly on site<sup>12</sup> with the FTIR open-path results. In Subsection 3.D we deal with N<sub>2</sub>O. First we derive local concentrations from open-path spectra. Then, by an analysis of solar absorption spectra of N<sub>2</sub>O, we derive the vertical column and an adjusted vertical volume mixing ratio

---

The authors are with the Fraunhofer-Institut für Atmosphärische Umweltforschung, Kreuzteckbahnstrasse 19, D-82467 Garmisch-Partenkirchen, Germany.

Received 22 April 1996; revised manuscript received 22 July 1996.

0003-6935/97/030735-07\$10.00/0

© 1997 Optical Society of America

(VMR) profile. From this information again we calculate a local concentration, which agrees with the open-path result.

FTIR open-path measurements have been widely used to gain path-integrated local concentrations at rural or industrial sites.<sup>13,14</sup> At the Zugspitze Observatory, to our knowledge for the first time, open-path experiments are performed in combination with solar absorption spectrometry at an Alpine site. New technical features implemented at the Zugspitze NDSC (Network for the Detection of Stratospheric Change) complementary site are described, and the analysis strategy of open-path and solar absorption spectra is presented.

## 2. Experiment

The main device of the Zugspitze open-path and solar absorption experiment is a Bruker IFS 120 HR spectrometer with a maximum resolution of  $\Delta\nu = 0.0015 \text{ cm}^{-1}$  (resolution is defined as  $\Delta\nu := 0.9/\text{optical path difference, or OPD}$ ). The optics of a 1.92-m Newtonian telescope (40-cm diameter) with a computer-controlled two-mirror solar tracker is matched to the spectrometer. For the open-path (or laboratory) experiment the radiation of three different internal sources can be directed through the telescope and solar tracker optics to an external retroreflector positioned at a horizontal distance of 123 m. The reflected radiation is then directed back into the spectrometer through a beam splitter. Internal sources (midinfrared, glow bar; near-infrared-visible, tungsten lamp; visible-ultraviolet, Xe lamp) as well as mirror coatings, beam splitters (midinfrared, KBr; near-infrared, Si on  $\text{CaF}_2$ ; visible, dielectric coating on quartz; ultraviolet, Al on quartz), and detectors (HgCdTe, InSb, Si diode, ultraviolet vacuum diode) are designed to cover a spectral range from  $600 \text{ cm}^{-1}$  to  $42\,000 \text{ cm}^{-1}$ . For the solar absorption experiment the solar tracker is shifted from the retroreflector direction to the solar direction by computer control.

For aliasing to be avoided and for zero line distortions from detector nonlinearity effects to be reduced, a set of six different optical narrow-band filters cover the HgCdTe and InSb spectral range ( $750\text{--}4500 \text{ cm}^{-1}$ ). A main advantage for the quality of the recorded spectra results from the spectrometer hardware control (Opus, Bruker) by means of a multitasking digital operation system. By this, subsequent interferograms can be continuously recorded without any time delay caused by the data-storing process. The continuous sampling during forward and backward motions of the scanner leads to an increased signal-to-noise ratio, especially in the case of the solar absorption experiment, in which the integration time is strongly limited because of the changing solar zenith angle.

The whole system is designed to minimize technical man power, e.g., the solar tracker is placed in a planetary dome (Baader Planetarium) opened and positioned automatically; the data of meteorological sensors (pressure  $\pm 2$  mbars, temperature  $\pm 0.5$  K,

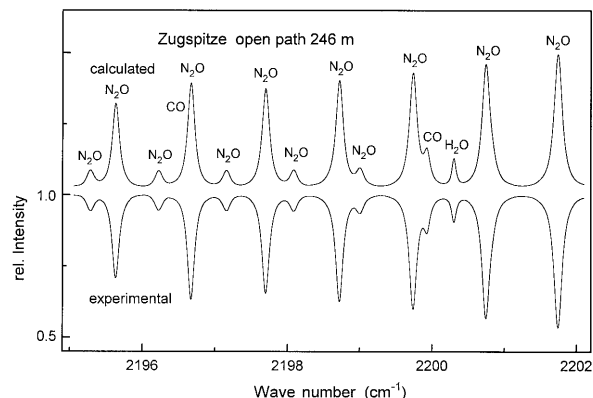


Fig. 1. Comparison of an experimental 246-m open-path spectrum recorded at the Zugspitze summit (2964 m a.s.l.,  $p = 703.4$  mbars,  $T = 266.45$  K) with an optical path difference of 30 cm (lower inverted trace) to a simulated spectrum (upper trace), showing vibration-rotation absorption features of  $\text{N}_2\text{O}$   $P9$  to  $P16$  transitions of the  $(0111) \leftarrow (0110)$  band and the (stronger)  $P24$  to  $P30$  transitions of the  $(0001) \leftarrow (0000)$  band, with significant interferences from CO ( $2196.664 \text{ cm}^{-1}$  and  $2199.931 \text{ cm}^{-1}$ ) and  $\text{H}_2\text{O}$  ( $2200.306 \text{ cm}^{-1}$ ).

humidity, wind, and rain) are stored in the spectral data files for scientific analysis and used for a shut-down protection of the optics in case of bad weather conditions.

## 3. Results and Discussion

### A. Data Recording

A typical open-path spectrum (246 m) at an altitude of 2964 m above sea level is displayed in Fig. 1, which has been recorded with the internal glow bar source and the liquid-nitrogen-cooled InSb detector. For a typical integration time of 1 h, a 1.3-mm-diameter Jacquinot aperture<sup>15</sup> (field of view, or FOV, 3.11 mrad), and a spectral resolution of  $0.03 \text{ cm}^{-1}$  (see definition above), a signal-to-rms-noise ratio of the order of 2000 can be achieved. A further increase of the aperture diameter toward the Jacquinot limit (2 mm for a resolution of  $0.03 \text{ cm}^{-1}$ ) would increase the signal-to-noise ratio at least to 4000 (even to 8000 in the case of the photon noise limit). Before Fourier transformation the interferogram was apodized (Norton-Beer, weak or medium<sup>16</sup>). For phase correction of the single-sided interferograms the Mertz method<sup>17</sup> was applied, with an optimized number of interferogram points. Parts of the spectrum used for spectral analysis were post-zero filled by a factor of 8. The signals in flat bottoms of completely saturated absorptions ( $\text{H}_2\text{O}$ ) were used to check the zero level. At this zero level, distortions in the open-path spectra of less than 0.15% of the signal in nearby absorption-free regions were found in the InSb range, even without optical filtering. However, in most backward scans, stronger zero line distortions have been found, which have to be analyzed in future research. For the results presented here, all backward scans were discarded.

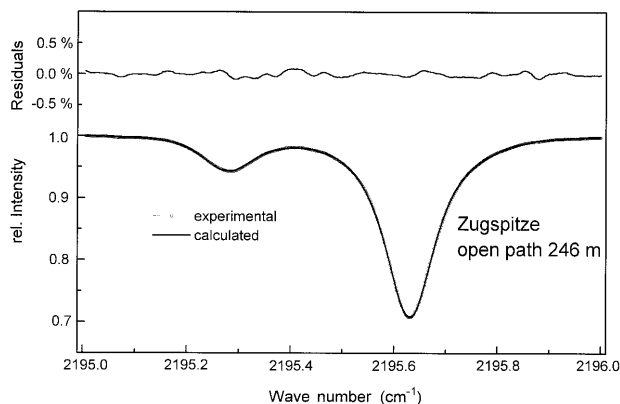


Fig. 2. Microwindow of the 246-m open-path spectrum of Fig. 1 used to derive the  $N_2O$  local concentration, showing experimental, SFIT simulation, and residuals (standard deviation, 0.039%) of the fitted range around the  $P16$  and  $P30$  transitions of the  $(0111) \leftarrow (0110)$  and  $(0001) \leftarrow (0000)$  bands, respectively.

### B. Spectral Analysis

In Fig. 2 the  $1\text{-cm}^{-1}$ -wide segment used for the spectral data analysis of  $N_2O$  is displayed on an expanded scale (also see Fig. 1). The weaker and stronger lines originate from the  $P16$  transition of the  $(0111) \leftarrow (0110)$  band, and the  $P30$  transition of the  $(0001) \leftarrow (0000)$  band, respectively. The result of nonlinear least-squares spectral curve fitting is displayed with its residuals (calculated minus observed). For the analysis the software package SFIT,<sup>2</sup> designed to analyze atmospheric multilayer problems (solar absorption), has been used with input files for pressure and temperature, VMR's, and optical path parameters that were reduced for the atmospheric one-layer problem. The model assumes a Voigt-type molecular line shape and uses the line-intensity and the pressure-broadening coefficients as input (1992 HITRAN database<sup>18</sup>; HITRAN is a high-resolution transmission molecular absorption database). Two major influences on the shape of the ILS are modeled from the input OPD and the Jacquinot FOV. Positions and intensities of the spectral features of as many as five different molecular species are simultaneously fitted along with one to three parameters to model the 100% transmission curve (for the small spectral intervals used in this study, only one to two background parameters were fitted).

Figure 2 shows that, for the lines of  $N_2O$  specified above, a fit to the noise level of the data is achieved (the standard deviation of the residuals is 0.039%). This means that all contributions to the experimental line shape and linewidth are modeled correctly. These contributions are (i) the molecular line shape modeled to be of the Voigt type, (ii) the contribution of the ILS, (iii) the atmospheric pressure along the open path (pressure broadening), and (iv) the temperature by means of the temperature dependence of the pressure-broadening coefficients. Discarding any accidental compensation between effects (i)–(iv), we find that Fig. 2 thus means that, according to (i), the assumption of a Voigt profile is correct. That is, no

motional narrowing effects such as Dicke narrowing<sup>19</sup> or line mixing<sup>20</sup> are present, which have often been observed in  $Q$  branches or at low densities.<sup>21</sup> Effects of this kind, which are not expected in the spectra shown here, would result in deviations from the Voigt profile, which have been implemented in the analysis of atmospheric spectra only recently.<sup>22</sup> According to (ii), the fact that the fitting residuals reflect only the experimental noise first means that there is no asymmetry distortion of the ILS caused by phase errors; furthermore, we correctly simulated the ILS by considering only the influences from the (limited) OPD and the Jacquinot FOV. In other words, there are no further contributions to the experimental ILS as, e.g., influences from an optical off-axis misalignment.

The SFIT software provides the possibility of fitting such further contributions to the ILS (other than the OPD and FOV) by fitting an effective apodization. This is a first-order approach in retardation space (linear ramp). The resulting effective apodization parameter is a measure of the strength of the fitted apodization (defined to display a value of 1.0 for box-car and 0.0 for triangular effective apodization). For our example of Fig. 2, the effective apodization fitting yields an effective apodization parameter of 0.982, which means that the spectrometer had been aligned almost perfectly during this experiment. Regarding (iii) and (iv), it should be stressed that the conditions for a perfect fit of the profile are correctly measured pressure and temperature. Typical of the gases discussed in this study, an error in pressure of 2 mbars leads to an error of only 0.3% in concentration; however, the effect of a (caused by wrong pressure) wrongly modeled pressure-broadened half-width can be sensitively seen from the fitting residuals. This can also be visualized in a change of the effective apodization parameter, because this parameter, of course, monitors *any* influence on the line shape, not only the instrumental one. By the temperature dependence of the pressure-broadening coefficients, an error in the measured temperature again results in a wrong half-width. By this, temperature errors of less than 1 K can be seen in the residuals.

### C. Horizontal Path Measurements: Comparison with *in situ* Data

In previous studies we analyzed the optimum spectral microwindows for the analysis of open-path spectra of various trace gases, as well as the corresponding detection limits attainable by a mobile remote-sensing system, including the K300 spectrometer (Kayser-Threde, Munich).<sup>14,23</sup> In Table 1 the Zugspitze local concentrations of  $CO$ ,  $CO_2$ , and  $CH_4$  derived from the high-resolution FTIR open-path measurements recorded with the Bruker IFS 120 HR spectrometer are compared with the simultaneously performed *in situ* measurements.<sup>12</sup> Thus we compare our path-integrated concentration measurements with point measurements performed only a few meters apart from one end of our open path. The 0.5-h mean values from several open-path spectra were compared with the VMR's determined from

**Table 1. Comparison of FTIR Open-Path Measurements with *in situ* Data of Local Trace-Gas Concentrations at the Zugspitze Summit**

FTIR Minus <i>in situ</i> Data	CO <sup>a</sup> (%)	CO <sub>2</sub> <sup>b</sup> (%)	CH <sub>4</sub> <sup>c</sup> (%)
$\bar{x}$	+4.3	-2.6	-0.4
$\sigma_x/\sqrt{n}$	0.4	0.3	0.2
$\sigma_x$	0.8	0.7	0.5

<sup>a</sup>The P11 transition (2099.083 cm<sup>-1</sup>) of the 1 4 0 band has been used.

<sup>b</sup>The P26 transition (2056.701 cm<sup>-1</sup>) of the (11101) 4 (00001) band has been used.

<sup>c</sup>The 3038.499 cm<sup>-1</sup> line of the (00011001) 4 (00000000) band has been used.

the *in situ* measurements. In all cases, mean relative differences  $\bar{x}$  (FTIR open path minus *in situ*) are below 4.3%, with the *in situ* VMR's being smaller for CO (+4.3% ± 0.4%), and higher for CO<sub>2</sub> (-2.6% ± 0.3%) and CH<sub>4</sub> (-0.4% ± 0.2%), respectively. This is a good agreement, considering the completely different approaches of the concentration analysis. The self-calibrated line-by-line Fourier-transform spectral data analysis directly yields the absolute concentration values, using only line parameters from laboratory investigations as input. In contrast, the *in situ* measurements do not directly yield absolute values, which is due to their measurement principles. For both CO<sub>2</sub> and CO, nondispersive infrared instruments were used; CH<sub>4</sub> was analyzed by means of a gas-chromatographic setup. The conversion of measured signals into mixing ratios is based on regular comparisons with precisely calibrated gas mixtures.<sup>12</sup> The errors in the mean relative differences ( $\sigma_x/\sqrt{n}$ , where  $n$  is the number of measured 0.5-h differences; Table 1) are well below mean relative differences  $\bar{x}$ . Thus even for the small number of data points analyzed, the derived mean relative differences are statistically significant and thus must be considered as (small) systematic deviations between open path and *in situ* measurements.

The errors of the FTIR open-path analysis are mainly of the systematic type. A typical random error is the error by the spectral noise on the derived horizontal column. However, this is only a negligible error of less than 0.15% for the example of N<sub>2</sub>O (Fig. 2). Further random errors result from the pressure and temperature measurements, with resulting errors in concentration below 1% for the species discussed here (for a check for the errors in pressure and temperature, see Subsection 3.B). An instructive way of studying the consistency of analyzing *one* line of each species (Table 1) is to derive the concentration of each molecular species by the analysis of several rotational lines. For the gases discussed here, the relative differences in the concentrations of different individual lines are of the order of 1%. Reasons for such relative deviations are (i) zero line distortions from detector nonlinearity, (ii) relative errors in the HITRAN line parameters, (iii) different relative temperature dependences, and (iv) varying problems from cross sensitivities (H<sub>2</sub>O) in different

spectral regions. Although zero line distortions have been checked to be below 0.15% of nearby absorption-free transmission levels (Subsection 3.A), the main systematic error source for the concentrations of N<sub>2</sub>O, CO, CO<sub>2</sub>, and CH<sub>4</sub> in the open-path spectra discussed here are the HITRAN line parameters. The line parameter error is determined mainly by the error in the line intensity, which translates linearly into a concentration error (2% for N<sub>2</sub>O, 5% for CO and CO<sub>2</sub>, and 3% for CH<sub>4</sub>). Compared with this, as a further systematic error, the absorption path length (246 ± 1 m) again linearly translates into the concentration error. Finally, as a way to check for the stability of the algorithm, the spectral micro-windows used for fitting around the individual target lines (Table 1) were varied; e.g., for the case of N<sub>2</sub>O the spectral interval was chosen either to cover only one line or two lines of different bands (Fig. 2). Furthermore, various combinations of fixed or free-running fitting parameters were used. The results of the different fitting runs of one spectrum were found to vary below 1% in the derived concentration.

The precision of the *in situ* measurements varied between approximately 5% or better for CO, 0.3% for CH<sub>4</sub>, and 0.1% for CO<sub>2</sub>. The accuracy of the *in situ* measurements is strongly dependent on the accuracy of the calibration standards. The calibration gases used for CO<sub>2</sub>, CO, and CH<sub>4</sub> were related to internationally accepted calibration scales. CO<sub>2</sub> VMR's are given in the World Meteorological Organisation X85 scale.<sup>24</sup> Because variance  $\sigma_x$  of the mean relative difference between the FTIR open-path and *in situ* concentrations is within the same order of magnitude (Table 1) as the precision of the *in situ* measurements, it can be concluded that the FTIR open-path reproducibility is comparable with that of the *in situ* measurements.

#### D. Local Concentrations from Vertical Profiles: Comparison with Horizontal Columns

Here we describe, for the example of N<sub>2</sub>O, a cross check between the local concentrations derived from a solar absorption experiment (Fig. 3) and a horizontal path experiment (Fig. 2). The basis of this kind of validation is that the absorption profile of a solar absorption experiment contains the information on the local concentration on site. For this it is necessary to derive information on the total vertical column as well as information on the relative vertical VMR distribution. This is comparably straightforward for the example of N<sub>2</sub>O, because the VMR as a function of height displays a nearly constant value (near 300 ppbv, where ppbv is parts in 10<sup>9</sup> by volume) up to a height of approximately 15 km and then decreases strongly and monotonously. This was already found in 1970,<sup>25</sup> based on the results obtained from balloonborne cryogenic whole air sampling and the subsequent gas-chromatographic analysis, as described by Fabian *et al.*<sup>26</sup> and Schmidt *et al.*<sup>27</sup>

In Fig. 3 the segment from 2439.2 to 2440.0 cm<sup>-1</sup> used for the analysis of the solar absorption by N<sub>2</sub>O [P26 transition of the (1200) 4 (0000) band] is dis-

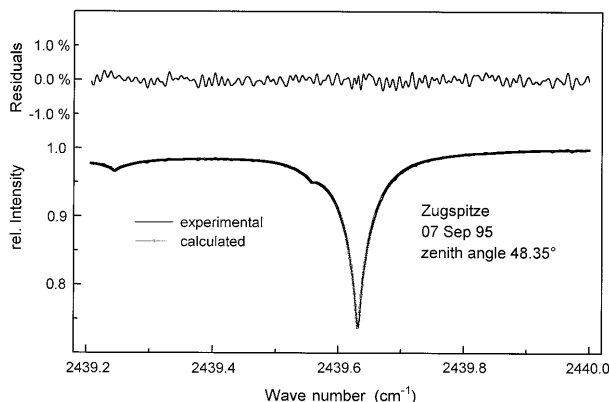


Fig. 3. Solar absorption spectrum of  $N_2O$  (zenith angle  $48.35^\circ$ ) recorded at the Zugspitze summit (2964 m a.s.l.) with an OPD of 175 cm, showing experimental, SFIT simulation, and residuals (standard deviation, 0.107%) of the fitted range around the  $P_{26}$  transition of the (1200) 4 (0000) band of  $N_2O$ . By vertical shifting and linear scaling of the VMR *a priori* profile, the residuals have been minimized for an effective apodization parameter with a value of 1.0 (see text for details). By this a local (tropospheric) concentration is derived from the solar spectrum that agrees with the open-path value (Fig. 2).

played together with the result of nonlinear least-squares spectral curve fitting by the SFIT software. In contrast to our use of the SFIT package for the horizontal path analysis with simplified input files for the one-layer problem, here we use the full 29-layer fitting capability. The input thus requires (i) a 29-layer pressure-temperature file as well as (ii) a 29-layer *a priori* vertical VMR profile, which is scaled by the fitting process by the same factor for all layers, *i.e.*, the relative *a priori* vertical distribution remains unchanged. Obtaining an adequate vertical pressure-temperature profile is not trivial compared with obtaining the local pressure-temperature data for the open-path analysis. Radiosonde data are available only twice a day from Munich (80 km to the north). However, there is the possibility of reducing the need for accurate atmospheric temperature profiles by choosing individual absorption lines with a small temperature dependence of the line intensity. The temperature dependence of the line intensity depends parametrically on the vibration-rotation ground-state energy,  $E''$ , of an infrared transition.<sup>28</sup> Thus a minimum temperature dependence corresponds to a specific  $E''$  value. The selected line centered at  $2439.632\text{ cm}^{-1}$  (Fig. 3) results from a transition with a lower state energy of  $294.06\text{ cm}^{-1}$  close to the ideal  $E''$  value, with a resulting mean temperature dependence of  $0.15\%\text{ K}^{-1}$  in the 240–280 K range. Therefore this line was selected by Zander *et al.*<sup>1</sup> in a recent study; however, a different line ( $1193.15\text{ cm}^{-1}$ ) was used for the analysis of a lower-resolution spectrum.<sup>29</sup> For our fitting standard, seasonal mean pressure-temperature profiles were used and compared with radiosonde data.

As outlined at the beginning of this section, for the derivation of local concentrations from a solar absorption line, both the total column and the rel-

ative vertical VMR distribution are required. Any substantial errors in the relative *a priori* VMR profile are seen from the fitting residuals deviating symmetrically around the center of the line from the noise level (strictly true for negligible pressure shift). Because of the simple structure of the vertical  $N_2O$  profile (see above), essentially two manipulations are sufficient to change a typical *a priori* profile toward the true profile within the experimental accuracy: (i) a linear scaling by the same factor for all vertical layers, and (ii) a vertical shifting, as reported in previous studies.<sup>1,30</sup>

It is interesting to point out the different meanings of the effective apodization parameter (Subsection 3.B) for the horizontal respective vertical column analysis. In case of the open-path experiment, this parameter contains information on possible instrumental misalignment or errors in the pressure or temperature; in case of the solar absorption experiment, the effective apodization parameter additionally contains information on deviations from the actual vertical VMR profile caused by varying pressure broadening in the different atmospheric layers and by varying influences of the temperature that are due to the temperature dependence of the pressure-broadening coefficients. Thus, forcing a fitting result of the solar spectrum (by means of manipulation of the *a priori* profile) to an effective apodization parameter close to the value of 1.0 yields at least strong evidence for having obtained a correct vertical VMR profile (assuming an accurate pressure-temperature profile and perfect optical alignment). For our experiment, by iterative vertical shifting and refitting (see above) of the standard atmospheric trace molecule spectroscopy profile, we could obtain a best fit with an effective apodization parameter close to the value of 1.0 (Fig. 3). For the solar spectrum measured coincident to the open-path spectrum of Fig. 2, this was achieved with a final vertical VMR profile shifted down 0.34 layers relative to the *a priori* profile (atmospheric 1-km layers up to a 15-km height; 2-km layers up to 32 km; 5-km layers up to 80 km). From the final fit of this VMR profile a linear scaling factor (the same factor for all layers) of 0.9976 relative to the *a priori* profile was obtained.

Because the analysis of a larger data set including trends of columns above Zugspitze is the subject of future research, we just briefly note that the column abundance measured for  $N_2O$  in November 1995 above Zugspitze (2964 m) is  $4.32 \times 10^{18}$  molecules  $\text{cm}^{-2}$ . The column abundance above Jungfraujoch Station (3580 m) has been systematically studied for years,<sup>1</sup> *e.g.*, for April 1992 it was found to equal  $3.87 \times 10^{18}$  molecules  $\text{cm}^{-2}$ . For direct comparison we consider the difference in the observation altitudes and calculate a column of  $3.81 \times 10^{18}$  molecules  $\text{cm}^{-2}$  above 3580 m at Zugspitze, which is the value to be compared with the Jungfraujoch values.

The retrieved vertical column abundance translates into a local  $N_2O$  concentration at the altitude of the Zugspitze Observatory equal to 307.2 ppbv, using the vertical profile obtained for an effective apodiza-

tion parameter of 1.0 (see above). This compares within 1% to the open-path result of 305.3 ppbv measured nearly at the same time. To check for a typical error, we find that shifting the vertical profile up or down by one layer from the best-fit level results in a change of  $\approx 1\%$  in the local concentration derived from the  $N_2O$  solar absorption spectrum. The implication of this good consistency is twofold. Neglecting any accidental compensations, both the multilayer radiative transport simulation is rather accurate, and the final vertical VMR profile is correct.

#### 4. Conclusions

We have investigated the species  $CO$ ,  $CO_2$ ,  $CH_4$ , and  $N_2O$  by means of FTIR open-path and solar absorption measurements. For the first three species, local concentrations could be derived that agree very well with the *in situ* results on site (relative difference below 4.3%). Compared with the *in situ* techniques, a disadvantage of the FTIR measurements is the demand for fair weather conditions (i.e., danger of optics damage). However, in addition to the multicomponent advantage (measurement of the different species during one measurement), the FTIR measurements have the advantage of being a path-integrating technique that is self-correcting for perturbations of the local concentrations from the infrastructure on site (e.g., restaurants, cable car power house). The results display a systematic type of the (small) concentration differences between open-path and *in situ* measurements. Further investigations with a larger data set, especially including an intercomparison at various different absolute concentration levels, may be used to decide whether the *in situ* calibration could be improved by the FTIR results, or whether the *in situ* results may be used to calibrate the FTIR measurements in the sense of possible refinements of molecular line parameters.

In a comparison with the horizontal path absorption of  $N_2O$ , we discussed the analysis of a  $N_2O$  solar absorption spectrum. By spectral analysis a vertical column together with an accurate vertical VMR profile could be obtained. These results from solar absorption were translated to a local concentration at the site level and thus were shown to agree very well (within 1%) with the open-path result. The main advantage from this combined analysis of horizontal and vertical columns is that horizontal path measurements provide significant information for the altitude profile retrievals. In subsequent research we will pursue the analysis of additional molecular species attainable by both open-path and solar absorption spectrometry.

The authors thank W. Seiler for his continuous interest in the progress of this study. They also thank the members of the Liège group, G. Roland, L. Delbouille, and R. Zander for their support during the buildup phase of the Zugspitze Observatory, and C. P. Rinsland (NASA Langley Research Center, Hampton, Va.) for providing the SFIT software package. We are indebted to H. E. Scheel for valuable

information and for making available the *in situ* data, and we thank A. Haak for valuable discussions. Funding of the Deutsche Bundesstiftung Umwelt is gratefully acknowledged.

#### References

1. R. Zander, D. H. Ehhalt, C. P. Rinsland, U. Schmidt, E. Mahieu, J. Rudolph, P. Demoulin, G. Roland, L. Delbouille, and A. J. Sauval, "Secular trend and seasonal variability of the column abundance of  $N_2O$  above the Jungfraujoch station determined from IR solar spectra," *J. Geophys. Res.* **99**, 16,745–16,756 (1994).
2. C. P. Rinsland, R. E. Boughner, J. C. Larsen, G. M. Stokes, and J. W. Brault, "Diurnal variations of atmospheric nitric oxide: ground-based infrared spectroscopic measurements and their interpretation with time dependent photochemical model calculations," *J. Geophys. Res.* **89**, 9613–9622 (1984).
3. A. Goldman, F. J. Murcray, F. H. Murcray, and D. G. Murcray, "Measurements of several atmospheric trace gases above the south pole in December 1986 from high-resolution 3–4  $\mu m$  solar spectra," *J. Geophys. Res.* **93**, 7069–7074 (1988).
4. F. J. Murcray, F. H. Murcray, and D. G. Murcray, "Infrared measurements of column abundances of several trace gases in the Antarctic atmosphere," *Rev. Geophys.* **26**, 81–88 (1988).
5. J. Notholt, A. Meier, and S. Peil, "Total column densities of tropospheric and stratospheric trace gases in the undisturbed arctic summer atmosphere," *J. Atmos. Chem.* **20**, 311–332 (1995).
6. W. A. Matthews, P. V. Johnston, D. G. Murcray, F. J. Murcray, and R. D. Blatherwick, "Column abundance of hydrogen chloride above Lauder, New Zealand," in *Ozone in the Atmosphere*, R. Bojkov and P. Fabian, eds. (Deepak, Hampton, Va., 1989).
7. N. S. Pougatchev and C. P. Rinsland, "Spectroscopic study of the seasonal variation of carbon monoxide vertical distribution above Kitt Peak," *J. Geophys. Res.* **100**, 1409–1416 (1995).
8. N. S. Pougatchev, B. J. Connor, and C. P. Rinsland, "Infrared measurements of the ozone vertical distribution above Kitt Peak," *J. Geophys. Res.* **100**, 16,689–16,697 (1995).
9. X. Liu, F. J. Murcray, and D. G. Murcray, "Comparison of HF and HCl vertical profiles from ground based high-resolution infrared solar spectra with halogen occultation experiment observations," *J. Geophys. Res.* **101**, 10,175–10,181 (1996).
10. L. D. Delbouille, "Issues affecting the photometric accuracy of a FTS," in *Fourier Transform Spectroscopy: New Methods and Applications*, Vol. 4 of 1995 OSA Technical Digest Series (Optical Society of America, Washington, D.C., 1995), p. 126.
11. W. Mankin, Report on the fifth meeting of the NDSC Infrared Working Group (Atmospheric Chemistry Division, National Center for Atmospheric Research, Boulder, CO, 1995).
12. H. E. Scheel, R. Sladkovic, and W. Seiler, "Aufbau und Betrieb einer Meßstation zur Bestimmung des Langzeitverhaltens klimarelevanter Spurenstoffe," Abschlußbericht zum Projekt 8272-622-52445 des Bayerischen Staatsministeriums für Landesentwicklung und Umweltfragen, Juni 1991.
13. C. P. Rinsland and A. Goldman, "Infrared spectroscopic measurements of tropospheric trace gases," *Appl. Opt.* **31**, 6969–6971 (1992).
14. R. Haus, K. Schäfer, W. Bautzer, J. Heland, H. Mosebach, H. Bittner, and T. Eisenmann, "Mobile Fourier-transform infrared spectroscopy monitoring of air pollution," *Appl. Opt.* **24**, 5682–5688 (1994).
15. P. R. Griffiths and J. A. de Haseth, *Fourier Transform Infrared Spectrometry* (Wiley, New York, 1986), Chap. VII.
16. R. H. Norton and R. Beer, "New apodizing functions for Fourier spectrometry," *J. Opt. Soc. Am.* **66**, 259–264 (1976); *J. Opt. Soc. Am.* **67**, 419 (1977), erratum.
17. L. Mertz, *Transformations in Optics* (Wiley, New York, 1965);

- “Auxiliary computation for Fourier spectrometry,” *Infrared Phys.* **7**, 17–23 (1967).
18. L. S. Rothman, R. R. Gamache, R. H. Tipping, C. P. Rinsland, M. A. H. Smith, D. C. Benner, V. Malathy-Davi, J.-M. Flaud, C. Camy-Peyret, A. Perrin, A. Goldman, S. T. Massie, L. R. Brown, and R. A. Toth, “The HITRAN molecular database: editions of 1991 and 1992,” *J. Quant. Spectrosc. Radiat. Transfer* **48**, 469–507 (1992).
  19. R. H. Dicke, “The effect of collisions upon the Doppler width of spectral lines,” *Phys. Rev.* **89**, 472–473 (1953).
  20. V. I. Alekseev and I. I. Sobel’man, “Influence of collisions on stimulated random scattering in gases,” *Sov. Phys. JETP* **28**, 991–994 (1969).
  21. R. Sussmann, T. Weber, E. Riedle, and H. J. Neusser, “Frequency shifting of pulsed narrow-band laser light in a multi-pass Raman cell,” *Opt. Commun.* **88**, 408–414 (1992).
  22. D. C. Benner, C. P. Rinsland, V. M. Devi, M. A. H. Smith, and D. Atkins, “A multispectrum nonlinear least squares fitting technique,” *J. Quant. Spectrosc. Radiat. Transfer* **53**, 705–721 (1995).
  23. K. Schäfer, R. Haus, J. Heland, and A. Haak, “Measurements of atmospheric trace gases by emission and absorption spectroscopy with FTIR,” *Ber. Bunsenges. Phys. Chem.* **99**, 405–411 (1995).
  24. H. E. Scheel, Fraunhofer Institut für Atmosphärische Umweltforschung, D-82467 Garmisch-Partenkirchen (personal communication, 1996).
  25. K. Schütz, C. Runge, R. Beck, and A. Albrecht, “Studies of atmospheric N<sub>2</sub>O,” *J. Geophys. Res.* **75**, 2230–2246 (1970).
  26. P. Fabian, R. Borchers, G. Flentje, W. A. Matthews, W. Seiler, H. Giehl, K. Bunse, F. Müller, U. Schmidt, A. Volz, A. Khedim, and F. J. Johnen, “The vertical distribution of stable trace gases at mid latitudes,” *J. Geophys. Res.* **86**, 5179–5184 (1981).
  27. U. Schmidt, G. Kulesa, A. Khedim, D. Knapska, and J. Rudolph, “Sampling of long lived trace gases in the middle and upper stratosphere,” in *Sixth ESA Symposium on European Rocket and Ballon Programmes* (European Space Agency, Noordwijk, 1983), pp. 141–145.
  28. L. R. Brown, C. B. Farmer, C. P. Rinsland, and R. Zander, “Remote sensing of the atmosphere by high resolution infrared absorption spectroscopy,” in *Spectroscopy of the Earth’s Atmosphere and Interstellar Medium*, K. Narahari Rao and A. Weber, eds. (Academic, San Diego, Calif., 1992), pp. 97–151.
  29. X. Liu and F. J. Murcray, “N<sub>2</sub>O vertical profiles from ground-based solar absorption spectra taken at McMurdo Station during austral spring of 1989,” in *Optical Remote Sensing of the Atmosphere* Vol. 2 of 1995 OSA Technical Digest Series (Optical Society of America, Washington, D.C., 1995), pp. 96–98.
  30. A. Barbe and P. Marché, “Obtention du profil de concentration de N<sub>2</sub>O à partir de mesures dans le domaine infrarouge faites à partir du sol,” *C R Acad. Sci. Paris*, **300**, 63–66 (1985).